Proceedings of the 1999 Antenna Applications Symposium, Monticello, IL, Sept. 15-17, 1999.

MEMS-SWITCHED RECONFIGURABLE MULTI-BAND ANTENNA: DESIGN AND MODELING

William H. Weedon and William J. Payne
Applied Radar, Inc. 14 Union Street, Watertown, MA 02472

Gabriel M. Rebeiz
Radiation Laboratory, University of Michigan, Ann Arbor, MI 48109

Jeff S. Herd and Michelle Champion
Air Force Research Laboratory, 31 Grenier St., Hanscom AFB, MA 01731

Abstract ? **Reconfigurable multi-band antennas are attractive for many military and commercial applications where it is desirable to have a single antenna that can be dynamically reconfigured to transmit and/or receive on multiple frequency bands. Such common-aperture antennas find applications in space-based radar, unmanned aerial vehicles (UAVs), communication satellites, electronic intelligence aircraft and many other communications and sensing applications. The reconfigurable antenna can be envisioned as an array of microstrip patch elements that are resonant at the highest operation frequency f_{max}, that can be connected together using switches to form groups of elements that are resonant at several lower frequencies $f_{max}/?_i$, where $?_i$, i= 1,2,…,N are scale factors related to the element groupings. It is easy to envision that an array that can be reconfigured to operate over a relative bandwidth of 100:1 would require hundreds and perhaps thousands of switches. Hence, a critical component of the reconfigurable antenna is the switches or relays used to interconnect the patch elements. Moreover, the efficiency (insertion loss) and effectiveness (isolation) of the switches will dictate the overall performance of the reconfigurable antenna array. One type of switch that has received a lot of attention recently as a candidate for reconfigurable antennas is the micro-electromechanical system (MEMS) switch. In this paper, we present design and modeling details for a prototype reconfigurable muli-band antenna using MEMS switches. A general adaptive reconfigurable (GARF) feed methodology is employed to allow various antenna configurations to have independent feed structures, and hence be tuned independently. We present computer simulations and measurement results for a small reconfigurable patch module (RPM) that may be used as a building block for a larger array in a tile architecture.**

1. Introduction

Antennas for many airborne vehicles such as UAV's, satellites and ELINT aircraft are required to satisfy a diverse range of requirements imposed by radar and communications systems in order to maximize the effectiveness of the aerial platform. It is highly desirable to have a single antenna that could be automatically reconfigured [1-16] to satisfy the frequency band and gain requirements of different applications. In this manner, several communications and remote sensing systems could utilize a common antenna aperture, resulting in considerable savings in size, weight and cost.

A typical example is in a space-based radar scenario, one may want to have a satellite antenna that can be dynamically reconfigured to provide SAR at X-band, communications at L-band, and AMTI radar at S-band. Another example is the Global Hawk UAV, where it would be desirable to have a single antenna aperture that could be reconfigured to provide communications from VHF to K-band, foliage penetration (FOPEN) radar from VHF to L-band, and SAR at X-band. There are many applications in both the military and commercial arenas where it would be desirable to combine the functionality of a number of antennas.

A key enabling technology for the successful development of reconfigurable multi-band antennas is the development of switches with low-loss, high-isolation and low bias power requirements. Below approximately 1 GHz, PIN diodes [11-12] are extremely efficient and are suitable switching elements. Above 1 GHz, various photonic switches have been proposed for microwave antenna applications [5-7,13-14], but have met limited success for one reason or another. Recently micro-electromechanical system (MEMS) switches have been receiving a lot of attention [1,2,15-16] as potential antenna switching elements.

MEMS switches have several characteristics that are attractive for reconfigurable antenna development. Among these are their inherent wide bandwidth, low insertion loss (~0.2 dB), and low bias current in both the ON and OFF states. The low bias current is due to the fact that the switch operates using electrostatic force. A voltage excitation is required to actuate the switch, but once actuated, the switches hold their ON/OFF state with very little bias power. Hence, these switches can be very efficient. Another advantage is that the MEMS devices are being manufactured using silicon IC batch-processing techniques, thereby leveraging previous investments in processing facilities.

While conceptually simple, the development of a reconfigurable phased-array antenna spanning several decades of frequency bandwidth poses several design

challenges. The first design decision is the choice of the antenna elements themselves. It is anticipated that some type of an antenna patch element would be used, due to their low profile and the fact that they can be fabricated easily using PC board techniques. The design of patch radiating elements for a given board material and thickness is fairly standard [17-19]. The real challenge is developing interconnection and feed structures to connect the antenna elements, switches, and phase shift elements together in such a way that the antenna may be reconfigured to meet the needs of various applications.

Another difficulty in developing multi-band antennas with wide separation between bands is achieving a large instantaneous bandwidth in each band, particularly at the low frequency band of operation. The element to ground-plane separation imposes a bandwidth limit at the lowest frequency band due to the close proximity of the element to the ground plane. When the elements are grouped together at low frequency to form an "effective patch" consisting of a grid of smaller elements there is an additional "element fill factor" that tends to limit bandwidth. At the upper frequency band of operation, surface waves are the limiting factor.

A general adaptive reconfigurable feed (GARF) methodology is proposed for designing reconfigurable multi-band antennas such that the feeds for the various configurations may be designed and tuned independently. A reconfigurable patch module (RPM) is proposed to be used as a building block for a larger array in a tile architecture. We present design, simulations and measurement results for a dual-mode RPM capable of operating at both S-band and X-band.

2. Background on MEMS Switches

An excellent review article on RF-MEMS devices is presented by Brown [1]. Essentially, the MEMS switch is a micromachined device consisting of a membrane or strip of metal suspended over an electrode. Activation of the switch is caused by an electrostatic field induced by an applied voltage. The main advantage of these devices is that once the switch is activated, there is almost no power required to hold the switch in the activated state. Hence, the MEMS switch is an extremely efficient device.

Current MEMS Switch designs employ one of three mechanical configurations: either the cantilever, air-bridge or diaphram [1]. The cantilever switch, illustrated in Figure 1, consists of a thin strip of metal and dielectric fixed at one end and suspended over an air gap. The air-bridge, illustrated in Figure 2, is a metal/dielectric strip that is fixed at both ends and suspended over an air gap in

the middle. The diaphram consists of a metal/dielectric membrane fixed around the edges and suspended over an air gap in the middle. The circuit configurations used by the MEMS switches can be either series or parallel. Contacts are either resistive (metal-metal) or capacitive (metal-insulator-metal).

Several MEMS switches have been investigated to date with varying degrees of success. Two of the more successful approaches [1] are 1) the cantilever switch with a series-connected metal-metal contact, similar to Figure 1; and 2) the air-bridge switch similar to Figure 2 with a parallel-connected metal-insulator-metal contact. Other mechanical configurations such as diaphrams have not been successful [1].

(a) OFF State (b) ON State

Figure 1: Illustration of cantilever MEMS switch.

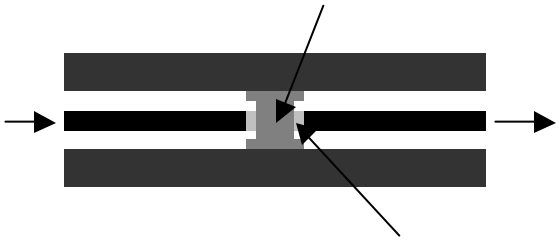

Figure 2: Illustration of air-bridge MEMS switch.

2.1 Series-Connected Cantilever Switch

Series-connected cantilever MEMS switch designs have been developed independently by both Hughes Research Lab., Malibu, CA and Rockwell Science Center, Thousand Oaks, CA. The operating principle is that electrostatic force created by an induced voltage is used to move a cantilever that series-connects the RF circuit. Both the Hughes and Rockwell switches have proven successful in achieving low insertion loss on the order of 0.2 dB from DC to 40 GHz in the ON

state and high isolation on the order of 30 dB DC ? 15 GHz and 20 dB 15 GHz ? 40 GHz in the OFF state. Both of these switches appear to be well-suited for reconfigurable antenna applications.

2.2 Parallel-Connected Air-Bridge

Another successful MEMS switch is the parallel-connected air-bridge switch. This switch was developed by Raytheon/TI, Dallas, TX. This switch utilizes a metal-insulator-metal bridge that in the ON state loads the center contact with a small capacitance (high impedance), and in the OFF state, shorts the center contact to ground with a high capacitance (low impedance). The insertion loss with the parallel air-bridge in the ON state is about 0.3 dB from DC ? 40 GHz, comparable to the series cantilever. The isolation in the OFF state, however, is rather poor for frequencies below 15 GHz. The OFF-state isolation shows a linear trend: 30 dB at 35 GHz, 20 dB at 15 GHz, 10 dB at 5 GHz, etc. This poor isolation at low frequency is due to the fact that the switch capacitance *Cs* shunts the characteristic impedance Zo of the transmission line. The isolation *ISO* can be determined from circuit theory as [1]

$$ISO = 10 \log_{10} [1+(? \; Zo \; Cs)^2].$$

Hence, as ? ? 0, *ISO* ? 0 dB.

Because of the inherent poor isolation of the parallel-connected air-bridge switches, we would expect that the series-connected cantilever switches would be more useful for reconfigurable antennas that operate below 15 GHz.

MEMS switches have several inherent limitations. The first limitation is switching speed, which is typically several microseconds [1,2]. This should not be a severe limitation, however, and would allow sufficient time for the antenna to be reconfigured for various communication and radar functions. A second problem with MEMS switches is mechanical "stiction" [1]. Since the MEMS device is mechanical in nature, the device parts can sometimes become bonded together upon physical contact. MEMS researchers are currently working vigorously to solve the stiction problem.

3. Reconfigurable Patch Module (RPM) Concepts

We now develop concepts for the reconfigurable patch modules (RPMs) that are essentially the building-blocks, or sub-array elements, in a reconfigurable antenna. The RPM utilizes one or more patch antenna elements in combination with MEMS switches to allow multi-frequency reconfiguration. Essentially, the

RPM is the fundamental building block in our reconfigurable antenna tile architecture.

We restrict our attention to microstrip patch antenna elements due to their low profile, low cost, low weight, and ease of fabrication. The antenna elements with potential for consideration are:

- ?? Rectangular Patch
- ?? Rectangular Resonant Patch Stack
- ?? Printed Circuit Dipole

The primary difference between the rectangular patch and the resonant patch stack is that the resonant patch stack has a broader bandwidth.

We could consider more "coarse-grain" elements with inherent broadband characteristics such as spiral antennas and linear log-periodic elements. However, we prefer to use the "fine-grain" microstrip patch elements because there is a greater degree of flexibility in terms of configuring the array for multi-frequency and phased-array applications using fine-grain elements. Another reason for not selecting spiral elements is that spiral antennas are inherently circularly polarized, whereas linear polarization is normally used for SAR.

The design of microstrip patch elements is rather straightforward, and can be found in many texts [17-19]. The design of a reconfigurable multi-band antenna, however, involves the combination of patch elements and MEMS switches in such a way that the antenna can be reconfigured to adapt to different frequency bands. Precisely how to connect these elements together such that the module has the desired frequency bandwidth, impedance, and radiation characteristics is the problem under consideration.

Figures 3–5 illustrate possible configurations of the antenna elements in the RPMs. Figure 3 [3?5] shows a printed dipole RPM, consisting of dipole segments series-connected with MEMS switches. By symmetrically switching in dipole segments on either side of the generator, the dipole resonant frequency is changed by a scale factor.

In Figure 4 [6], a single rectangular patch is series connected with a MEMS switch to another patch segment to tune the patch. The concept of tuning a single patch with additional patch segments could be extended to include several patch segments, and hence be reconfigured for a wide range of frequency bands.

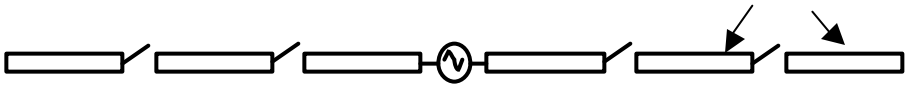

(a) RPM resonant at frequency f_0

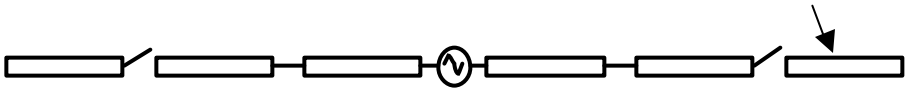

(b) RPM resonant at frequency f_0 / 2

(c) RPM resonant at frequency f_0 / 3

Figure 3: Printed dipole reconfigurable patch module (RPM). Printed circuit dipole segments are connected by series MEMS switches. Closed MEMS switches are indicated by solid lines connecting dipole segments. Dipole is fed by a generator at the center.

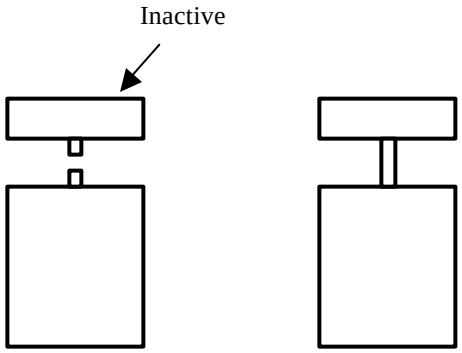

(a) MEMS switch open; (b) MEMS switch closed

Figure 4: Single rectangular patch reconfigurable patch module (RPM). (a) RPM resonant at frequency f_0; (b) RPM resonant at frequency f_0 / p where p is a scale factor. RPM consists of two rectangular microstrip patch elements of different size connected by a transmission line and series MEMS switch.

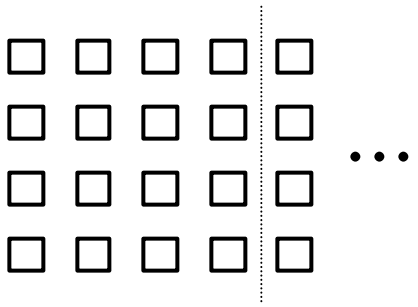

(a) RPM resonant at frequency f_0. All patch elements are active.

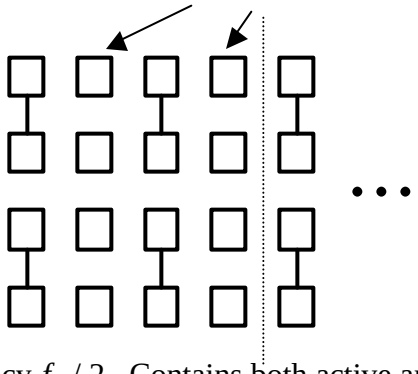

(b) RPM resonant at frequency f_0 / 2. Contains both active and inactive elements.

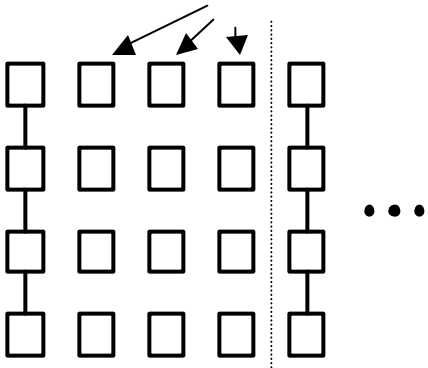

(c) RPM resonant at frequency f_0 / 4. Contains both active and inactive elements.

Figure 5: 4×4 Microstrip patch reconfigurable patch module (RPM). All antenna patch elements are assumed to be connected with MEMS switches. Solid line between elements indicates a closed switch, no line indicates an open switch. Dashed line separates the RPM modules.

Figure 5 illiustrates a 4×4 element microstrip patch RPM [1]. This RPM uses a symmetric 4×4 array of patch elements, where each patch is series-connected to each adjacent patch in the vertical direction with an MEMS switch. With all of the switches open, the array is resonant at frequency f_0. When two elements are connected together as in Figure 4(b), with a column of inactive elements separating each pair on connected elements, the array is vertically polarized and resonant at frequency $f_0 / 2$. Similarly, if four elements are connected together as in Figure 4(c), with three rows of inactive elements separating each row of active elements, the result is a vertically polarized array resonant at fequency $f_0 / 4$. Note that the second row of active elements would actually be located on an adjacent RPM in a tile architecture.

The RPM configurations considered in Figures 3–5 each have inactive elements in certain configurations. For example, in Figure 3(a) there are four inactive dipole segments when the dipole is resonant at frequency f_0. In figure 4(a), the patch segment is disconnected from the main patch element, and is hence inactive. In Figure 5 (b) and (c), the 4×4 patch array has columns of inactive patch elements when the array is resonant at frequency $f_0 / 2$ and $f_0 / 4$, respectively.

The examples considered in Figures 3–5 illustrate possible configurations or conceptual starting points for RPM design. Each of these designs has its own merits and advantages and disadvantages. The square or rectangular microstrip element array appears at first to be the most general and attractive configuration. However, practical design experience has shown that there are certain limitations of this approach. For example, it is difficult to obtain a large bandwidth at the low frequency band due to the height of the element above the ground plane. Another limitation is that the rectangular patch configuration is somewhat limited in the selection of frequency band due to the discrete number of patches and finite element separation. The segmented patch concept illustrated in Figure 4 may be conbined with a rectangular patch array to allow fine-tuning of the frequency band center frequency. Dipole patch arrays may offer some additional benefits as well.

4. General Adaptive Reconfigurable Feed (GARF) Methodology

Once the antenna elements themselves are chosen and designed, the RPM is not complete unless we have a method of feeding the elements with the appropriate excitation amplitude and phase in the various configurations. In addition, impedance matching must be done in order to minimize reflection loss. The design of corporate feed structures for microstrip patch arrays is straightforward [17–20]. What complicates the design is that either the same feed mechanism

must work for all array configurations, or the feed mechanism must adapt as the array is reconfigured.

Although it is possible conceptually, it is not likely that the same feed structure will be used for all array configurations. In a simple, canonical design, it is conceivable to get away with a single corporate feed. But practical design experience dictates that feed linewidths and lengths will need to be tuned in order to maximize the performance of the antenna. The likelihood that this tuning, or impedance matching, will be valid for all array configurations in a more complicated design is very small.

A more general feed design is to use an approach whereby multiple feed transmission lines are run in parallel beneath the active antenna elements. Vias are placed at selected points to bring the appropriate feed line to the appropriate microstrip patch element at the surface in the proper feed location. MEMS switches are placed directly on the patch elements themselves to connect the patch element feed points (typically somewhere on the interior of the patch elements, about 1/3 from the edge for a rectangular patch) to the feed vias. This arrangement is illustrated in Figure 6. We call this new method of feeding the antenna elements the general adaptive reconfigurable feed (GARF).

A second advantage to using the GARF approach is that it allows for a method of properly terminating unused elements in the array. That is, in addition to the parallel feed transmission lines beneath the antenna element plane, we could have several termination lines connected with various load termination impedances. As the array is reconfigured, MEMS switches will connect the unused antenna elements to vias that lead to the appropriate termination line as illustrated in Figure 7.

The GARF method conceptually provides a method of feeding the RPMs and array elements in such a way that the feed mechanism is adaptive. Each array configuration has its own feed transmission line that may be individually tuned for optimal performance. It also allows a mechanism for properly terminating unused array elements in the various configurations.

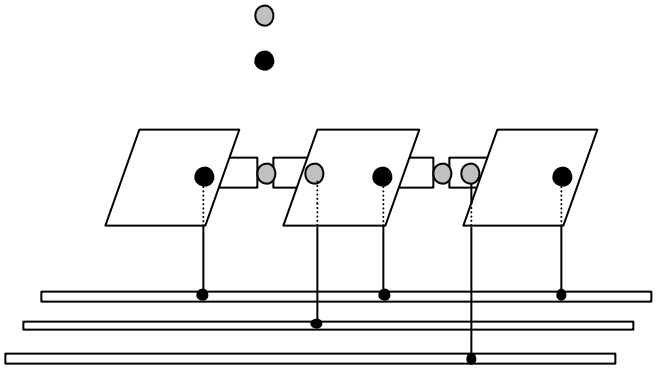

(a) RPM resonant at frequency f_0. Patches fed via Feed-1.

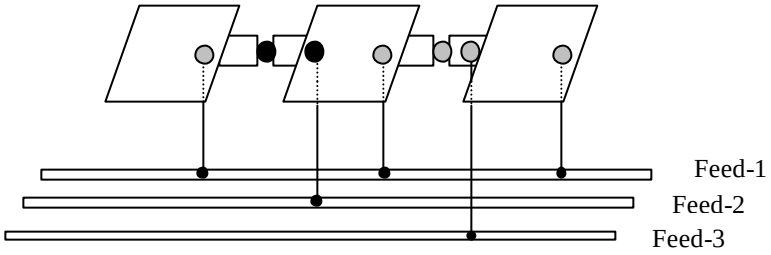

(b) RPM resonant at frequency f_0 / 2. Patches fed via Feed-2.

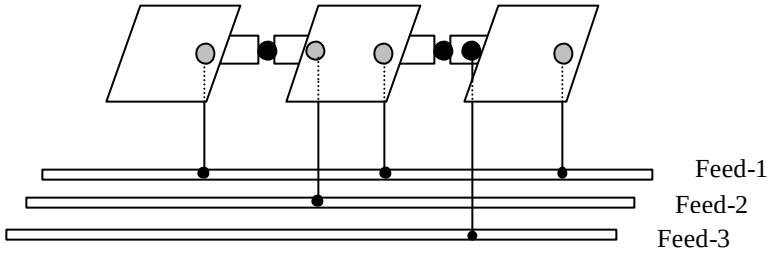

(c) RPM resonant at frequency f_0 / 3. Patches fed via Feed-3.

Figure 6: Illustration of General Adaptive Reconfigurable Feed (GARF) design for feeding multi-frequency reconfigurable antennas. Design allows each array configuration to be fed independently, simplifying impedance matching procedure.

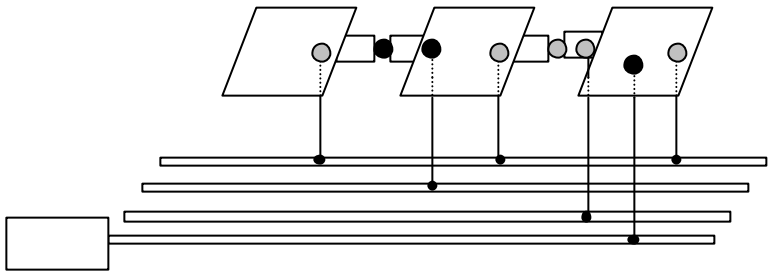

Figure 7: Illustration of General Adaptive Reconfigurable Feed (GARF) design for terminating unused elements in multi-frequency reconfigurable antennas.

5. Design, Simulation and Measurement Results

A prototype RPM was developed to operate at two distinct and widely-separated frequency bands. Our design goal was to develop and antenna that resonated at roughly 2 GHz (S-band) and 10 GHz (X-band). A square microstrip element resonating at 10 GHz was chosen as the basic antenna element. The 10 GHz patch elements were then connected together using thin microstrip lines to form the 2 GHz "effective element". Since MEMS switches were not available at this early stage, a microstrip line with or without a small gap was used to represent an OPEN or CLOSED switch.

Rogers RT/duroid 5880 material ($?_r$=2.2, tan?????) was chosen as the substrate due to its low dielectric constant and loss tangent. Two substrate thicknesses were investigated: .062" and .125". Computer simulations were utilized to compute the input impedance, return loss and radiation patterns of the antenna. Several prototypes were built and tested using the .062" substrate. The .125" dielectric is currently on back-order. Therefore, measurement results are presented only for the .062" substrate.

Our initial design philosophy was to start with a square patch element on the .062" substrate, where the patch dimensions were designed to resonate at roughly 10 GHz. The patch elements were probe-fed from the bottom. The initial probe location was determined approximately using a cavity model. A more accurate computer simulation was then performed using HFSS.

5.1 Results for .062" substrate

We began by designing a single patch resonant at 10 GHz (X-band). A square patch was used with dimension .364" square on the .062" substrate. The patch was probe-fed from the bottom. The probe position was initially determined using a cavity model, then fine-tuned with HFSS. The optimized probe position was .062" from the center of the patch. Figures 8–10 show the HFSS and measured impedance, return loss and radiation patterns for the single patch. Note that there is a slight difference between the simulation and measured center frequency (9.38 GHz vs. 9.82 GHz). We believe that the simulation is limited in its ability to accurately model the resonance frequency. The measured bandwidth is 4.28% versus 4.7% for the simulation. The phase rotation between the simulation and measured smith-chart impedance is due to the electrical length of the probe feed. There was no attempt to optimize the center of the resonance frequency, since this could be trivially done by adjusting the size of the patch.

Figures 11-13 show similar simulation and measurement results for an open 3x1 patch array. In Figure 11(a), we see that the array consists of three patches identical to the single patch discussed above. The feed location is the same. Note that there are now .040" lines extending from each patch with an .050" gap to simulate an OPEN MEMS switch. The simulated and measured center frequency for the antennas are 8.48 GHz and 8.955 GHz. Note that there is a significant drop in both the simulated and measured center frequency, due to the addition of the .040" open transmission lines, which detune the patches. Again, the simulation underestimates the resonance frequency. The measured bandwidth of 4.13% was actually larger than the simulated value of 3.5%. This could be due to the higher center frequency for the measured data and the error due to the discrete simulated frequency step size.

Figures 14 and 15 show simulated and measured data for the closed 3x1 array. No radiation patterns were measured for this antenna due to the low frequency limit of the anechoic chamber. In Figure 14(a), we see that the .050" gap in the .040" transmission lines connecting the patches is now removed, simulating a CLOSED MEMS switch. The simulated and measured center frequencies are 1.905 GHz and 1.8527 GHz. Here, the simulation overestimates the resonance frequency. The simulated and measured bandwidths are 0.2% and 0.05%. These bandwidths are not acceptable for most applications, and would need to be increased. Part of the reason for this low bandwidth is that we constrained the OPEN and CLOSED feed locations to be the same. Note in Figure 15(a) that there is not a good impedance match for the CLOSED antenna. The simulated impedance match in Figure 14(b) is not a bad match, however.

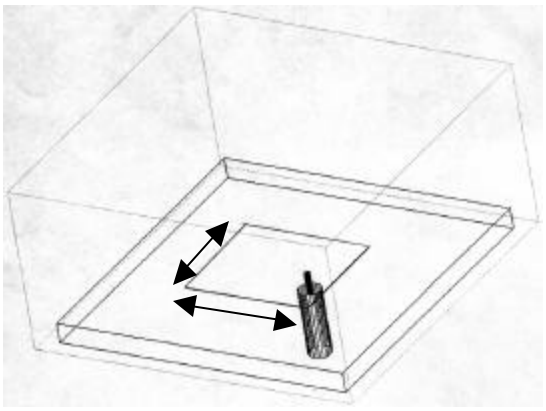

(a) Simulation Layout

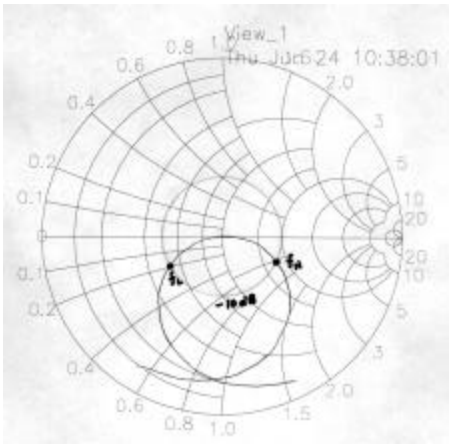

(b) Input Impedance

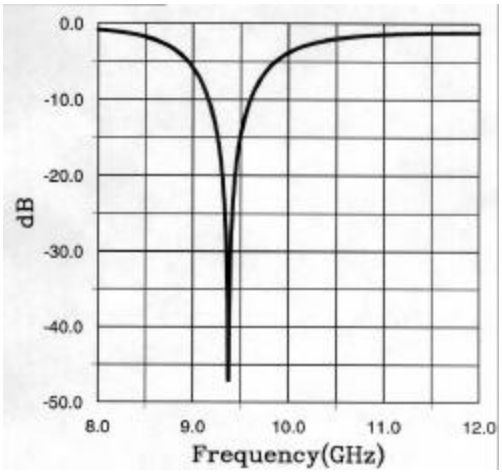

(c) Return Loss

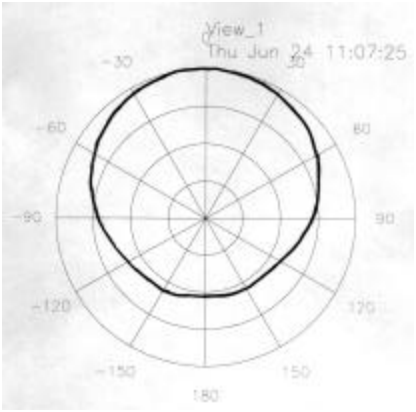

(d) Radiation Pattern

Figure 8: Simulation results for a single X-band patch. Bandwidth: f_L= 9.16 GHz; f_H= 9.60 GHz; BW= 4.7%.

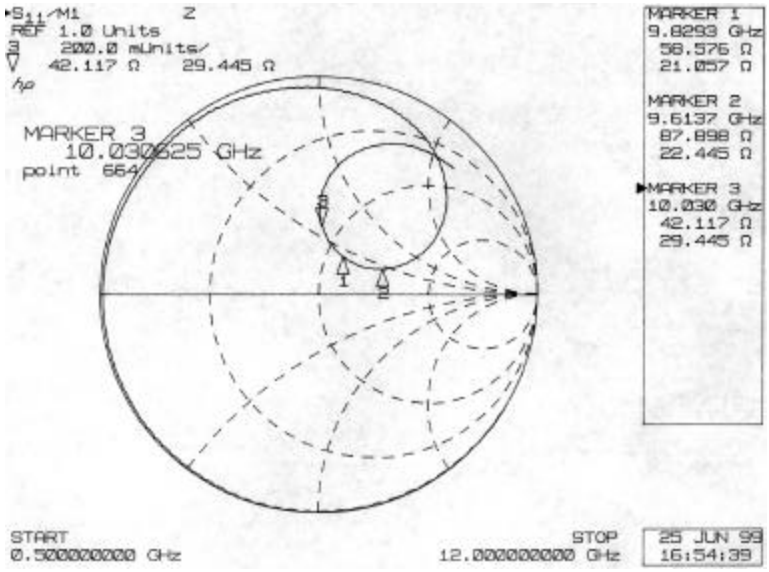

(a) Input Impedance

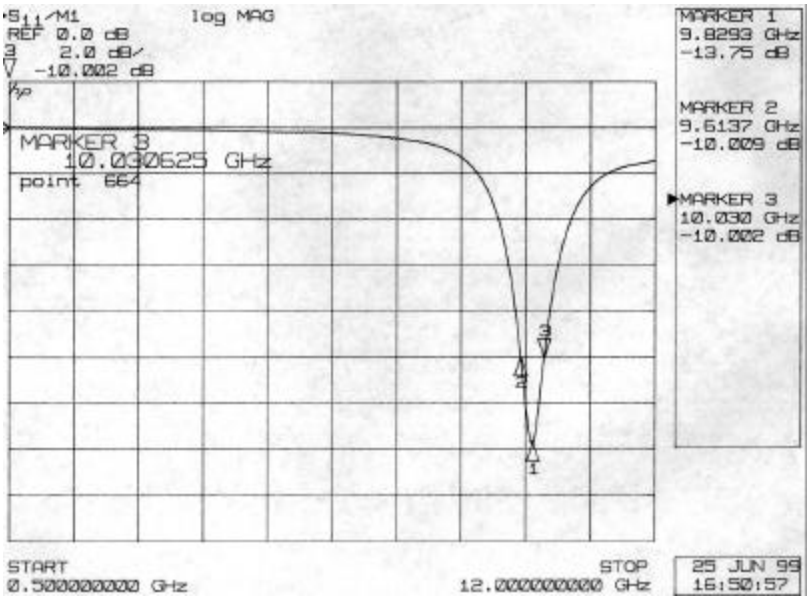

(b) Return Loss

Figure 9: Measured impedance and return loss for a single X-band patch. Bandwidth: f_L= 9.61 GHz; f_H= 10.03 GHz; BW= 4.28%

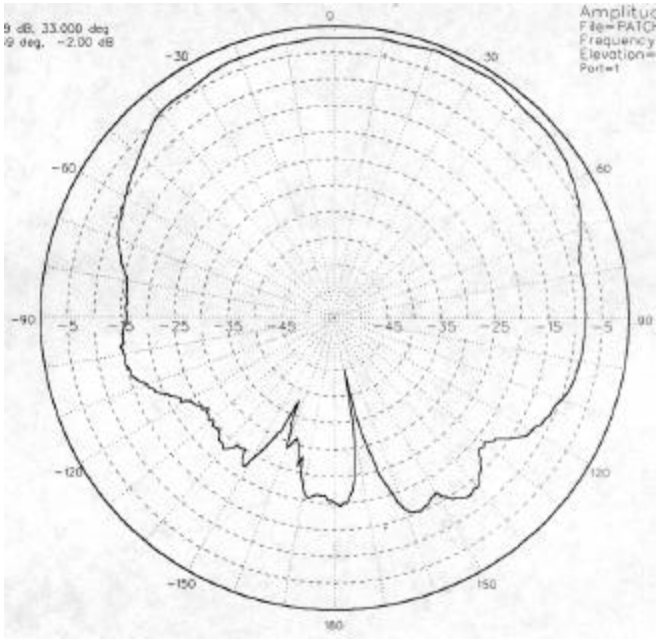

(a) E-Plane Pattern

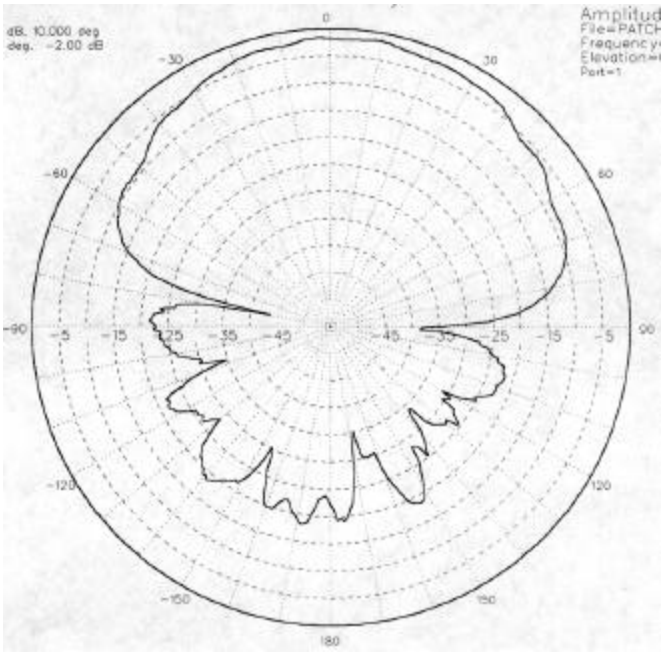

(b) H-Plane Pattern

Figure 10: Measured radiation patterns for single X-band patch. Amplitude is normalized to near 0dB at boresight.

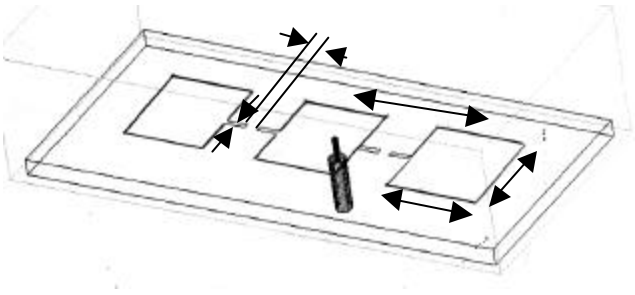

(a) Simulation Layout

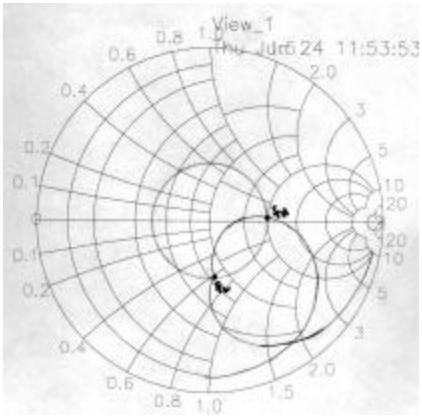

(b) Input Impedance

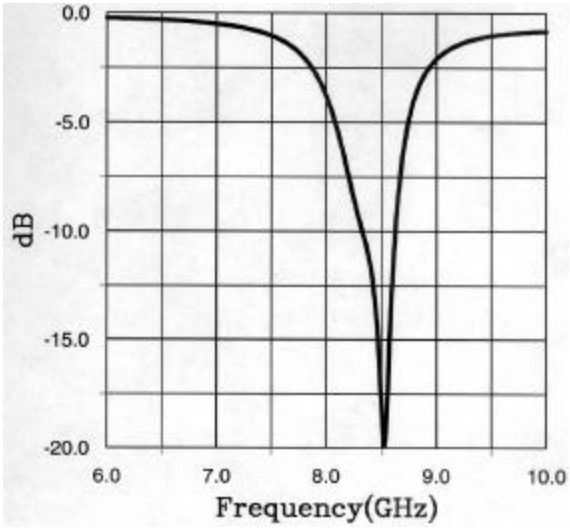

(c) Return Loss

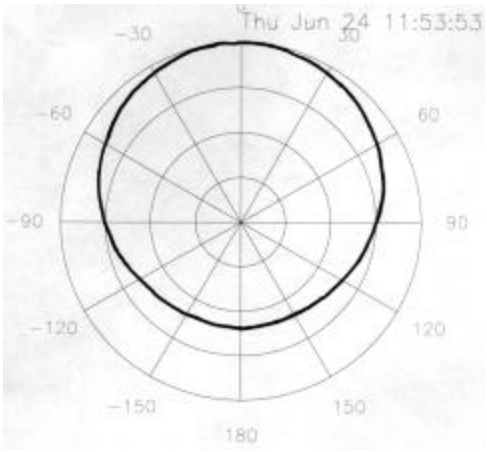

(d) Radiation Pattern

Figure 11: Simulation results for an open 3x1 patch array resonant at X-band. Bandwidth: f_L= 8.33 GHz; f_H= 8.63 GHz; BW= 3.5%.

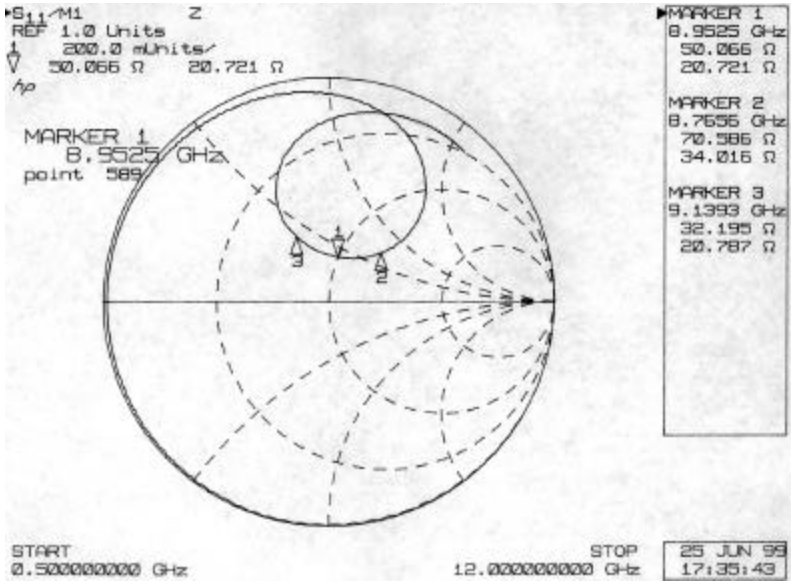

(a) Input Impedance

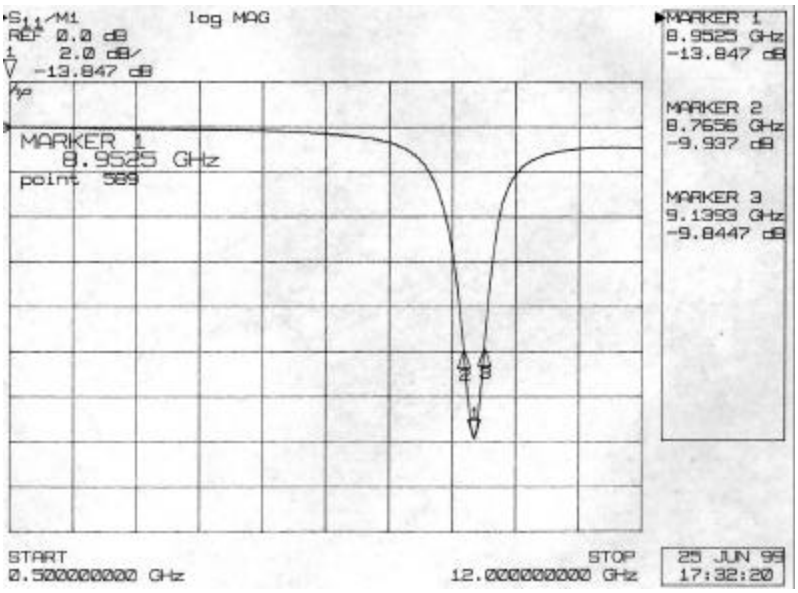

(b) Return Loss

Figure 12: Measured impedance and return loss for an open 3x1 patch array resonant at X-band. Bandwidth: f_L= 8.77 GHz; f_H= 9.14 GHz; BW= 4.13%.

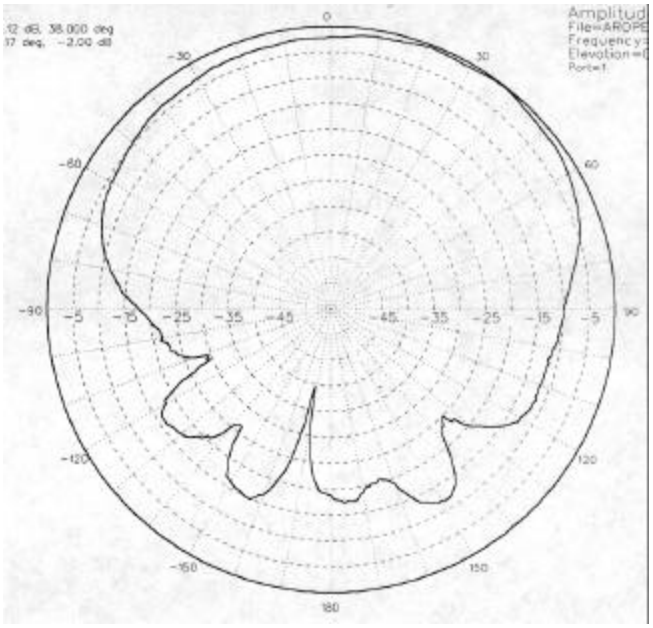

(a) E-Plane Pattern

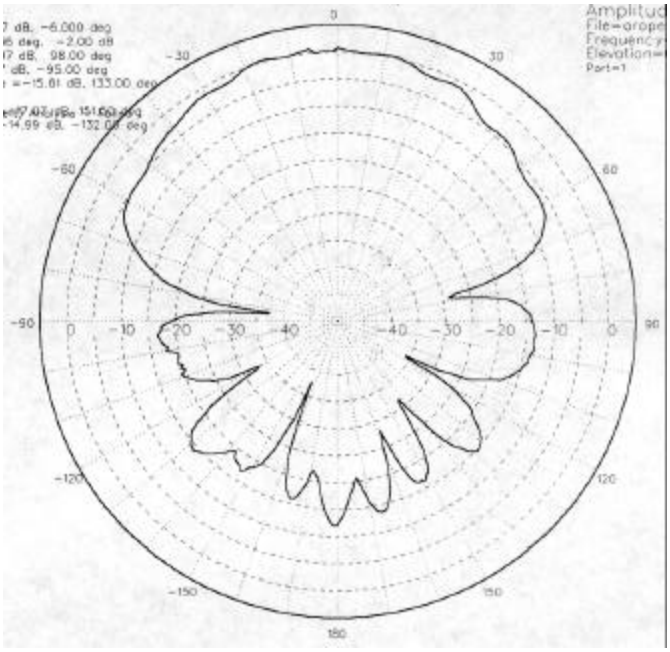

(b) H-Plane Pattern

Figure 13: Measured radiation patterns for an open 3x1 patch array resonant at X-band. Amplitude is normalized to near 0dB at boresight.

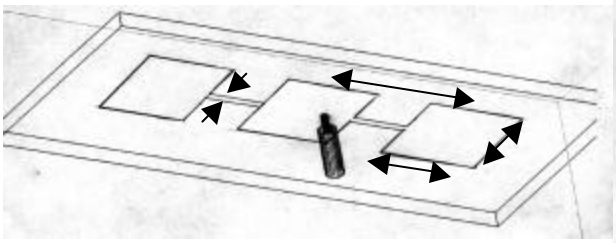

(a) Simulation Layout

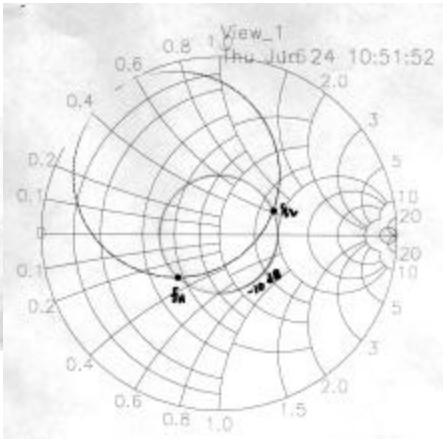

(b) Input Impedance

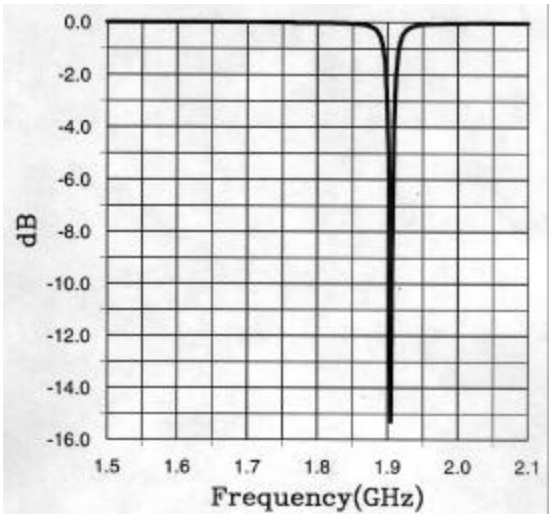

(c) Return Loss

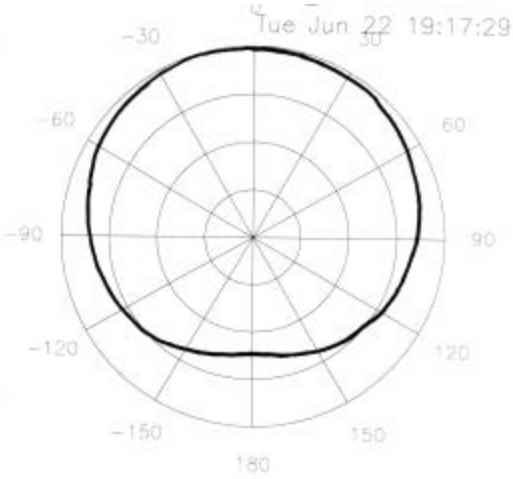

(d) Radiation Pattern

Figure 14: Simulation results for a closed 3x1 patch array resonant at S-band. Bandwidth: f_L= 1.903 GHz; f_H= 1.907 GHz; BW= 0.2%.

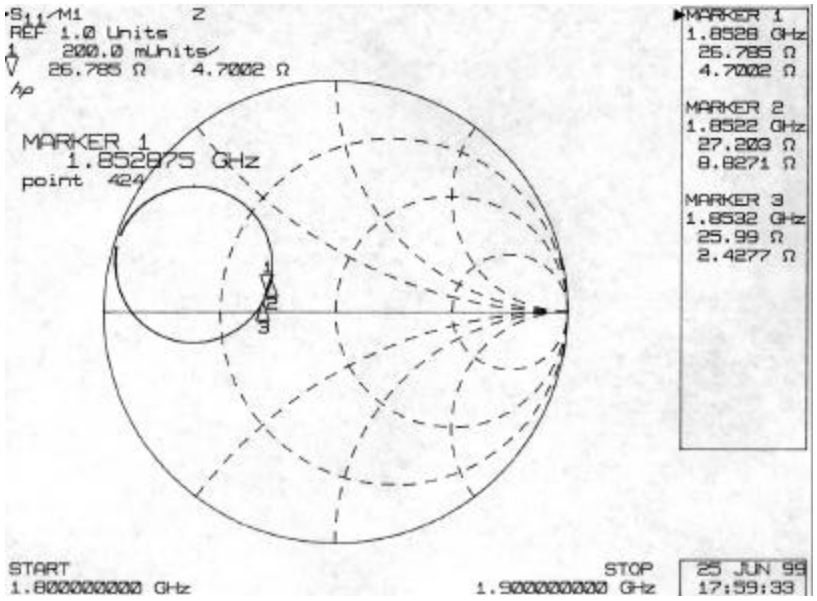

(a) Input Impedance

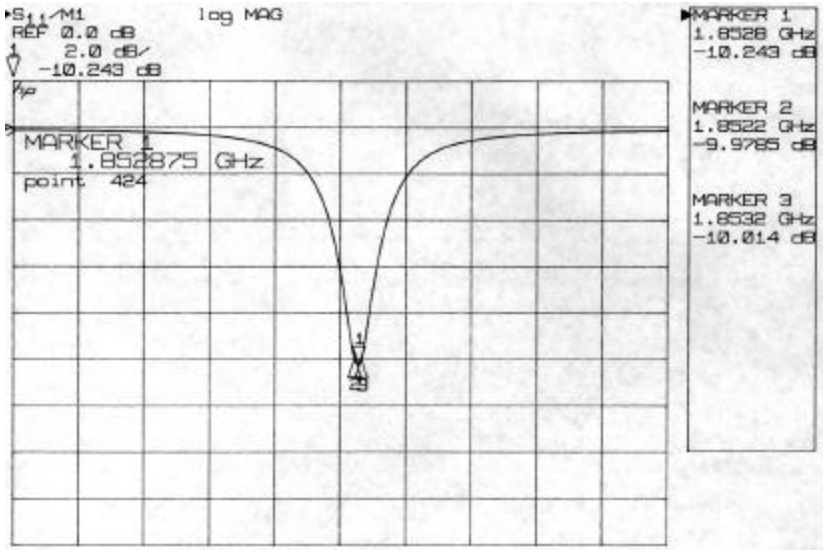

(b) Return Loss

Figure 15: Measured impedance and return loss for a closed 3x1 patch array resonant at S-band. Bandwidth: f_L= 1.8522 GHz; f_H= 1.8532 GHz; BW= 0.05%.

From the results above, it is evident that it is difficult to achieve adequate bandwidth at the low frequency band. Our initial hypothesis was this is due strictly to the height of the antenna elements above the ground plane. Further investigation proved otherwise. From Pozar [21, Fig. 1, p.158], the bandwidth of a rectangular patch at 2 GHz on .062" substrate should achieve approximately 1% bandwidth. Our simulated bandwidth (good impedance match) was a factor of 5 lower than this value, while our measured bandwidth (poor impedance match) was a factor of 20 below this value. To verify that a 1% bandwidth is achievable in practice, we built up a simple 2 GHz square patch on the .062" substrate. The patch dimensions were 1.97"x1.97" with the feed probe located .364" from the center. The measured impedance and return loss data are shown in Figure 16. We actually achieved a bandwidth of 1.22% with very little effort.

Evidently, the bandwidth limit at low frequency is not determined by the height of the microstrip substrate alone. Most likely, the bandwidth is also limited by the volume of the effective microstrip cavity resonator. The reduced volume of the "effective patch" apparently increases the Q of the resonant circuit, reducing the bandwidth. Using this reasoning, a 3x3 patch array should have a higher bandwidth than the 3x1 array.

5.2 Results for .125" substrate.

In order to increase the bandwidth at the low frequency band, we decided to experiment with .125" thick substrate. The results were computed using HFSS. General trends are similar to the .062" substrate data, with at least double the bandwidth. Measured results are not yet available at time of publication, since the substrate material is on backorder.

We first considered an X-band patch of dimension .350"x.350" fed .165" from the center, or .010" from the edge. Figure 17 shows the simulated input impedance and return loss. The 10dB bandwidth is greater than 1 GHz, or 10%.

Next, a 2 GHz square patch antenna was simulated to determine the maximum practical bandwidth achievable on the .125" substrate. The patch dimensions were 1.6"x1.6" with the feed probe .300" from the center. The computed bandwidth was 2.47%.

A single narrow rectangular patch was developed next to simulate the effect of a reduced resonator volume. The patch dimensions were 1.530"x.350". The probe location was .095" from the patch center. The measured bandwidth was .941% (f_L= 2.536 GHz; f_H= 2.560 GHz).

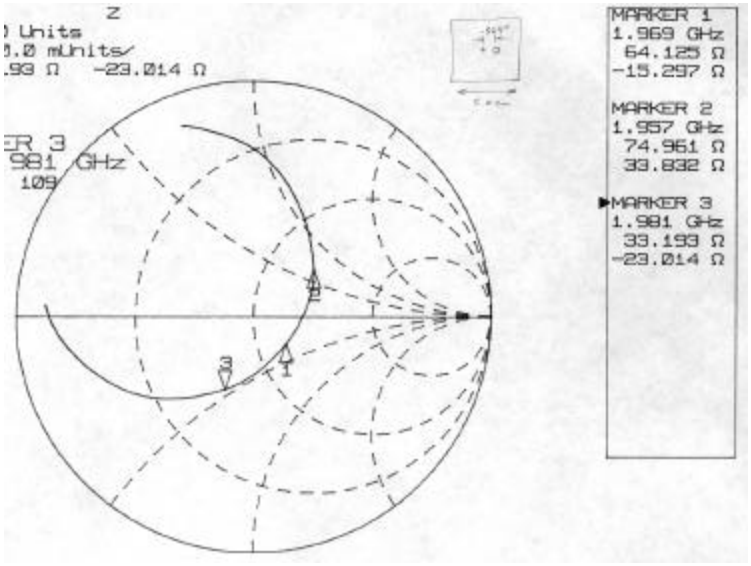

(a) Input Impedance

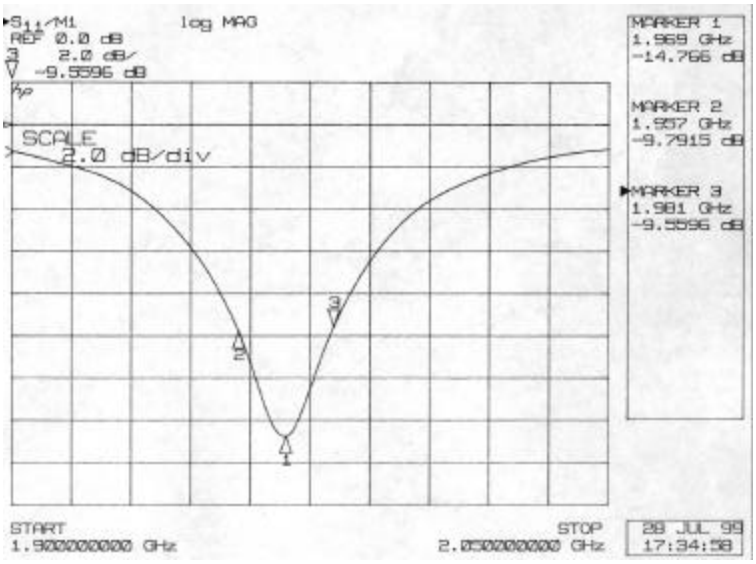

(b) Return Loss

Figure 16: Measured impedance and return loss for a square patch antenna resonant at S-band. Bandwidth: f_L= 1.957 GHz; f_H= 1.981 GHz; BW= 1.22%.

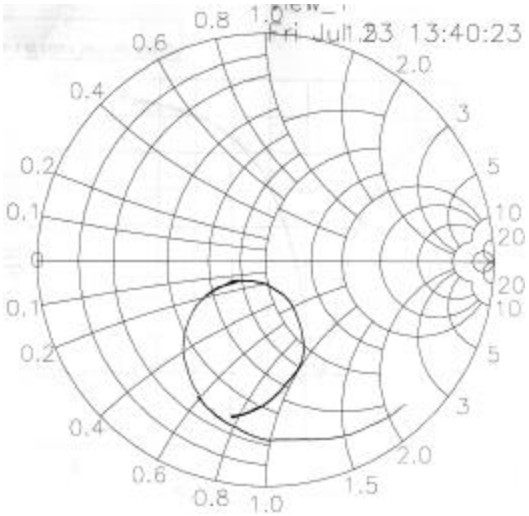

(a) Input Impedance

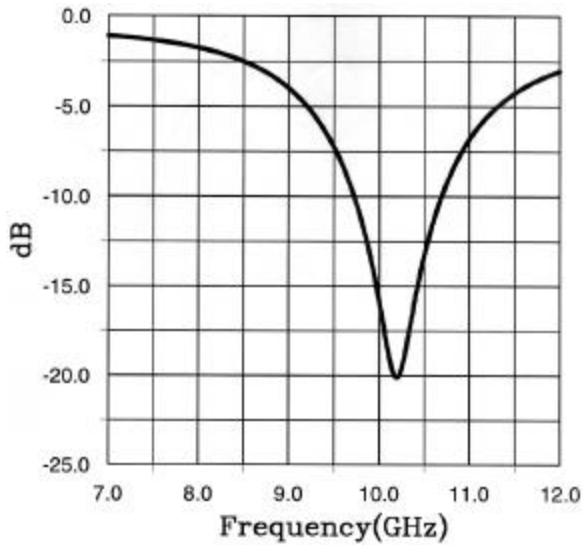

(b) Return Loss

Figure 17: Measured impedance and return loss for a square patch antenna resonant at X-band on .125" substrate. Bandwidth > 10%.

A closed 3x1 array of patches was simulated next on the .125" substrate. The basic patch elements were .350"x.350", with .040" connecting microstrip lines. The patches were separated by .590" on center. The center patch was fed .070" from the center. The measured bandwidth for the closed 3x1 array .519% (f_L= 1.92 GHz; f_H= 1.93 GHz).

Finally, a 3x3 closed patch array simulated using the .125" substrate. The results are shown in Figure 18. Figure 18(a) shows a diagram of the simulation layout. The patches are .370"x.370". After many simulation runs, it was determined that the optimal feed location was located .200" from the center of the center patch, which is actually located on the .040" microstrip line. Hence, the optimal feed location for the closed 3x3 array is actually not located on the patch elements themselves, but on the interconnecting microstrip line. This antenna had a 20 MHz bandwidth at 2 GHz, or roughly 1% bandwidth.

The simulation results for the .125" substrate are summarized in Table 1 below.

Table 1: Summary of Simulation Results for .125" Substrate

Configuration	**Dimensions**	**Probe Location**	**Percent B.W.**
X-Band Patch	.350x.350	.165	>10%
L-Band Square Patch	1.60x1.60	.300	2.47%
L-Band Narrow Rectangular Patch	1.53x.350	.095	.94%
L-Band CLOSED 3x1 Array	.350x.350	.070	0.52%
L-Band CLOSED 3x3 Array	.370x.370	.200	1.0%

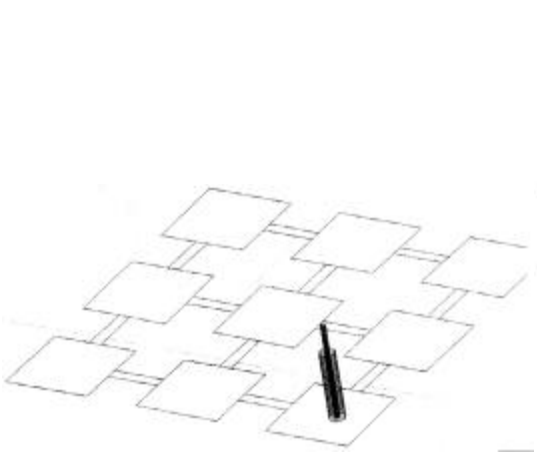

(a) Simulation Layout

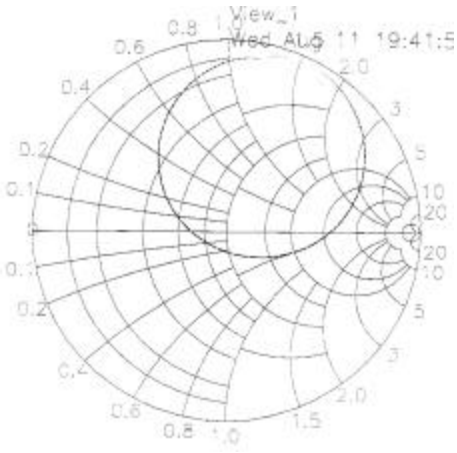

(b) Input Impedance

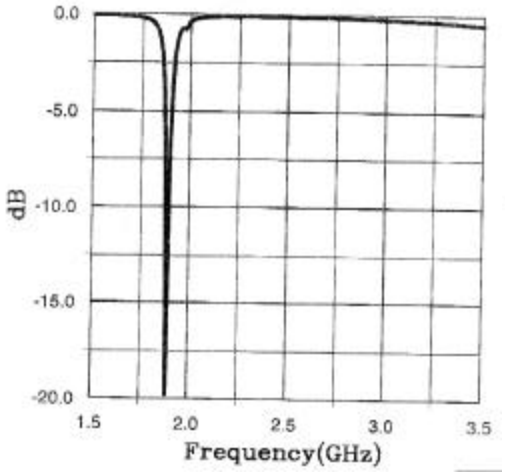

(c) Return Loss

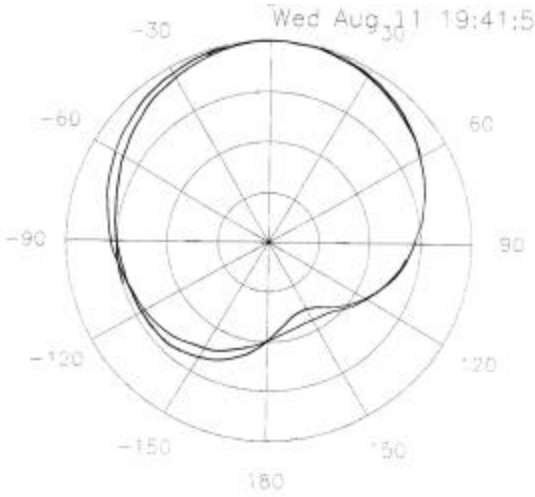

(d) Radiation Pattern

Figure 18: Simulation results for an open 3x3 patch array resonant at S-band on .125" substrate. Bandwidth: 1.0%

6.0 Conclusions

A general procedure was developed for designing reconfigurable multi-band antennas utilizing reconfigurable patch modules (RPMs) as basic elements in a tile architecture. A general adaptive reconfigurable feed (GARF) design methodology was proposed for designing and tuning the feed structure for each configuration independently. MEMS switches were discussed as possible switching elements due to their extremely low bias current and low insertion loss.

Design, simulation and measurement results were presented for a dual-mode RPM capable of operating at 10 GHz (X-band) and 2 GHz (S-band). Results were presented for both .062" and .125" thick substrate. Practical experience illustrates the difficulty of achieving a high relative bandwidth at the low frequency band. The bandwidth is limited by both the height of the element above the ground plane and the "element fill factor" determined by the volume of the resonant cavity of the "effective patch". Nevertheless, we have shown that it is possible to design a dual-mode RPM with 1% relative bandwidth at 2 GHz and 10% relative bandwidth at 10 GHz.

Since the MEMS switches are not currently available in packaged form, our current research is limited simulating the MEMS switches as ideal switches, and building separate antennas to simulate the OPEN and CLOSED configurations. We expect that samples of the MEMS switches will be available in the very near future, at which time we will incorporate these switches into our simulations and prototypes.

Acknowledgement

Support for this work is provided by a Phase-I Small Business Innovative Research (SBIR) contract from the U.S. Air Force Research Laboratory, Sensors Directorate, under contract F19628-99-C-0056.

References

[1] E. R. Brown, "RF-MEMS Switches for Reconfigurable Integrated Circuits," *IEEE Trans. Microwave Theory Tech.*, Vol. 46, No. 11, pp. 1868?80, Nov. 1998.

[2] N. S. Barker and G. M. Rebeiz, "Distributed MEMS True-Time Delay Phase Shifters and Wide-Band Switches," *IEEE Trans. Microwave Theory Tech.*, Vol. 46, No. 11, pp. 1881?90, Nov. 1998.

[3] R. C. Dempsey and R. M. Bevensee, "The Synaptic Antenna for Reconfigurable Array Applications – Description," *IEEE Antennas and Propagat. Society Symposium Digest*, pp. 760?3, 1989.

[4] R. M. Bevensee and R. C. Dempsey, "The synaptic Antenna for Reconfigurable Array Applications – Behavior," *IEEE Antennas and Propagat. Society Symposium Digest*, pp. 764?7, 1989.

[5] J. L. Freeman, B. J. Lamberty and G. S. Andrews, "Optoelectronically Reconfigurable Monopole Antenna," Electronics Lett., Vol. 28, No. 16, pp. 1502?3, July, 1992.

[6] A. S. Daryoush, K. Bontzos and P.R. Herczfeld, "Optically Tuned Patch Antenna for Phased Array Applications," *IEEE Antennas and Propagat. Society Symposium Digest*, pp. 361?4, 1986.

[7] M. L. Van Blaricum, "Photonic Antenna Reconfiguration: A Status Survey," *Proc. of the SPIE, Photonics and Radio Frequency II*, (San Diego, CA) July 21-22, 1998.

[8] D. Schaubert, F. Farrar, S. Hayes, and A. Sindoris, "Frequency-Agile, Polarization Diverse Microstrip Antennas and Frequency Scanned Arrays," US Patent #4,367,474, Jan. 4, 1983.

[9] D. Schaubert, and F. Farrar, "Microstrip Antenna with Polarization Diversity," US Patent #4,410,891, Oct. 18, 1983.

[10] F. Farrar and D. Schaubert, "Selectable-Mode Microstrip Antenna and Selectable-Mode Microstrip Antenna Arrays," US Patent #4,379,296, Apr. 5, 1983.

[11] R. Olesen, et. Al., “Quadrifilir Helix Antenna Tuning Using PIN Diodes,” US Patent #4,554,554, Nov. 19, 1985.

[12] P. Bhartia and I. Bahl, "Broadband Microstrip Antennas with Varactor Diodes," US Patent # 4,529,987, July 16, 1985.

[13] K. Turk, "Digitally Reconfigurable Antenna," *Proceedings of the 1996 Antenna Applications Symposium*, Allerton Park, Monticello, IL, Sept. 18-20, 1996.

[14] R. Gilbert, G. Pirrung, D. Kopf, P. Hoefler, F. Hayes, Structurally-Integrated Optically-Reconfigurable Antenna Array, *Proceedings of the 1995 Antenna Applications Symposium*, Allerton Park, Monticello, IL, 1995.

[15] J. J. Lee, D. Atkinson, J. J. Lam, L. Hackett, R. Lohr, L. Larson, R. Loo, M. Matloubian, G. Tangonon, H. De Los Santos, and R. Brunner, “MEMS Antenna Systems: Concepts, Design and System Implications,” *Nat. Radio Science Meeting*, (Boulder, CO), 1996.

[16] J. S. Herd and M. Davidovitz, “Reconfigurable Microstrip Antenna Using MEMS Switches”, submitted to Electronics Letters, April 1999.

[17] D. M. Pozar, *Microwave Engineering*. Reading, MA: Addison Wesley, 1990.

[18] D. M. Pozar and D. Schaubert Eds., *Microstrip Antennas: The Analysis and Design of Microstrip Antennas and Arrays.* New York, NY: Institute of Electrical and Electronics Engineers, 1995.

[19] C. A. Balanis, *Antenna Theory, Second Ed*. New York: Wiley, 1996.

[20] R. J. Mailloux, *Phased Array Antenna Handbook*. Norwood, MA: Artech House, 1994.

[21] D. M. Pozar and D. Schaubert, “A Review of Bandwidth Enhancement Techniques for Microstrip Antennas” in *Microstrip Antennas: The Analysis and Design of Microstrip Antennas and Arrays*, D. M. Pozar and D. Schaubert Eds. New York, NY: Institute of Electrical and Electronics Engineers, 1995.